Stability Analysis of Complex Multibody Systems

Olivier A. Bauchau and Jielong Wang

Daniel Guggenheim School of Aerospace Engineering, Georgia Institute of Technology, 270 Ferst Dr., Atlanta, GA 30332, USA

Abstract

The linearized stability analysis of dynamical systems modeled using finite element based multibody formulations is addressed in this paper. The use of classical methods for stability analysis of these system, such as the characteristic exponent method or Floquet theory, results in computationally prohibitive costs. Since comprehensive multibody models are "virtual prototypes" of actual systems, the applicability to numerical models of the stability analysis tools that are used in experimental settings is investigated in this work. Various experimental tools for stability analysis are reviewed. It is proved that Prony's method, generally regarded as a curve fitting method, is equivalent, and sometimes identical, to Floquet theory and to the partial Floquet method. This observation gives Prony's method a sound theoretical footing, and considerably improves the robustness of its predictions when applied to comprehensive models of complex multibody system. Numerical and experimental applications are presented to demonstrate the efficiency of the proposed procedure.

Key words: Multibody systems, Stability analysis, Prony's method

1 Introduction

An important aspect of the dynamic response of flexible multi-body systems is the potential presence of instabilities. The instability of a cantilevered beam subjected to a tip, compressive follower force [1], or the instabilities appearing in rotor dynamics [2,3] are but two well-known types instabilities that can occur in dynamical systems and flexible multi-body systems. If the equations of motion of the system can be cast in the form of linear, ordinary differential equations with constant coefficients, classical stability analysis methodologies based on the characteristic exponents of the system can be used. On the other hand, when the equations of motion of the system are cast in the form of linear, ordinary differential equations with periodic coefficients, Floquet theory [4,5] is used. Stability analysis is typically performed on simplified models with the smallest number of degrees of freedom required to capture

the physical phenomenon that causes the instability. As the number of degrees of freedom used to represent the system increases, these methods become increasingly cumbersome, and quickly unmanageable.

Due to increased available computer power, the analysis of flexible multi-body systems relies on increasingly complex, large scale models. Full finite element analysis codes are now routinely used for this purpose [6,7,8]. These codes should provide increasingly reliable predictions of the dynamic response of multi-body systems and stability can be assessed from the response of such simulations. If the response to an initial perturbation grows in time, the system is unstable, on the other hand, if the response decays, the system is stable. Unfortunately, this approach only provides qualitative results: it is difficult to compute damping rates from the response. Furthermore, this approach is prone to errors: if the system is not simulated for a long enough period, an unstable system could be mistaken for a stable one, or vice versa. Consequently, stability analysis methodologies are needed that can extract stability information and damping rates from large scale simulation tools.

Section 2 of this paper will review a number of existing tools for stability analysis, in an attempt to identify the methods that are most suitable for the stability analysis of complex multibody systems. Section 3 introduces the notational conventions used in the presentation of Prony's method that appears in section 4. The relationship of Prony's method to Floquet theory is discussed next, and practical implementation issues are addressed in section 5. Numerical examples are presented in section 6, and the conclusions of this study are drawn in the last section.

2 Tools for Stability Analysis

This section reviews existing methods for stability analysis, that can be arranged in three categories. First, *analytical methods* asses the stability characteristics of a dynamical system from the analytical expression of its governing differential equations. These methods form the basis for *numerical methods* that extract stability characteristics from numerical models that represent, as accurately as possible, the behavior of the dynamical system. Finally, *experimental methods* extract stability characteristics of the system from measured experimental data, such as signals from sensors that measure the response of the dynamical system. The advantages, shortcomings, limitations and range of application of the various approaches are discussed next.

The Lyapunov direct method [4] is the most general method for stability evaluation of a dynamical system written in the form $\dot{\underline{X}} = \underline{F}(\underline{X}(t))$, where t denotes time, $\dot{(\bullet)}$ a derivative with respect to time, $\underline{X}(t)$ the degrees of freedom of the system and $\underline{F}$ an arbitrary function of $\underline{X}$. Without loss of generality, it can be assumed that $\underline{F}(0) = 0$; under this convention $\underline{X}(t) = 0$ is an equilibrium solution. In Lyapunov direct method, the stability criterion involves a positive definite scalar function $V(\underline{X})$ such that $V(0) = 0$, called the *Lyapunov function*. If the following condition is satisfied, $\dot{V}(\underline{X})\ \underline{F}(\underline{X}) \leq 0$, then the solution $\underline{X}(t) = 0$

is Lyapunov stable. If the last condition is changed to $\dot{V}(\underline{X})\ \underline{F}(\underline{X}) < 0$, then the solution is asymptotically stable. The proof of this theorem can be found in [4].

The Lyapunov direct method enables assessing the stability characteristics of general dynamical systems. Unfortunately, the choice of the Lyapunov function is not always easy; in fact, there exist no general method of constructing a this function for nonlinear or time-dependent dynamical systems. Consequently, the Lyapunov direct method is an important theoretical tool, but it is not often used in practice. Clearly, the Lyapunov direct method is an analytical method that cannot be applied to numerical models or experimental data.

The characteristic exponent method [4] deals with the special case of dynamical systems defined by a set of linear, ordinary differential equations with constant coefficients. The dynamical system is governed by N first-order differential equations, $\dot{\underline{X}} = A\ \underline{X}$, where A is a matrix of constant coefficients. The solution of this system is known to be in the form of $\underline{X}(t) = \bar{\underline{X}}\ e^{\lambda t}$, and direct substitution into the governing equations leads to an eigenvalue problem $A\ \bar{\underline{X}} = \lambda\ \bar{\underline{X}}$. The stability characteristics of the system can be assessed from the eigenvalues, $\lambda_i,\ i = 1, 2, \ldots, N$, of matrix A. The damping ζ_i and frequency ω_i associated with each eigenvalue are $\zeta_i = \Re(\lambda_i)$ and $\omega_i = \Im(\lambda_i)$, respectively. The system is stable if all damping values are negative or zero, *i.e.* $\zeta_i \leq 0,\ i = 1, 2, \ldots, N$. The characteristic exponent approach is an analytical method that can be used for systems featuring a very small number of degrees of freedom; it is also used for numerical problem since the resulting eigenproblem is easily solved numerically for larger dimensional problems. The characteristic exponent method is also used to study the stability of small perturbations about a nonlinear equilibrium configuration of the system. First, the system is linearized about one of its nonlinear equilibrium solution, then, the characteristic exponent method is applied to the resulting linear system. For small systems, the linearization process can be carried out analytically; for larger systems, finite difference concepts are used for the linearization, but the computational cost becomes overwhelming as N increases.

Floquet theory [4,5] considers more general dynamical systems described by a set of N linear, ordinary differential equations with periodic coefficients of the form $\dot{\underline{X}} = A(t)\ \underline{X}$, where $A(t + T) = A(t)$ is a periodic matrix and T the period of the system. Note that constant coefficient systems, $A(t) = A$, are a special case where the period is arbitrary. Floquet theory involves the *transition matrix*, $\Phi(t, T)$, that relates the states of the system at time t and $t+T$, $\underline{X}(t+T) = \Phi(t, T)\ \underline{X}(t)$. In practice, the transition matrix is constructed by considering a full set of linearly independent solutions, $\Psi(t) = [\underline{X}_1(t), \underline{X}_2(t), \ldots, \underline{X}_N(t)]$. It then follows that $\Psi(t + T) = \Phi(t, T)\ \Psi(t)$ and $\Phi(t, T) = \Psi^{-1}(t)\Psi(t + T)$. The eigenvalues of the transition matrix are denoted $Q_i,\ i = 1, 2, \ldots, N$, and assumed to be distinct in this discussion; a complete discussion of the general case of repeated eigenvalues is found in ref. [4]. The stability criterion can now be stated as: the periodic system is stable if and only if the norm of all eigenvalues is smaller than unity: $|Q_i| < 1,\ \ i = 1, 2, \ldots, N$. The general solution of the periodic system can be written as

$$\underline{X}(t) = \sum_{i=1}^{N} \underline{A}_i(t)\ e^{\lambda_i t}, \tag{1}$$

where $Q_i = \exp(T\lambda_i)$.

This approach has been widely used for the assessment of stability of systems with periodic coefficients: general systems [1,9,10], rotor dynamics problems [2,3], and rotorcraft problems [11,12]. This discussion clearly shows the difficulties associated with the application of Floquet theory for stability assessment. Analytical applications are nearly impossible except for system featuring a very small number of degrees of freedom. In numerical applications, the evaluation of the transition matrix can become an overwhelming task as it requires one integration of the system of equations for an entire period, for each degree of freedom of the system. As the number of degrees of freedom of the system increases, this computational effort becomes prohibitive. In experimental application, it is not possible, in practice, to excite the system with N independent initial conditions, and it is impossible to measure all the states in the response. Hence, Floquet theory is not used in experimental applications.

To remedy this situations, the implicit Floquet theory [13,14] was developed. In this approach, the dominant eigenvalues of the transition matrix are computed using the Arnoldi algorithm, *without the explicit computation of this matrix*. This implicit method yields stability information at a far lower computational cost than that of the classical approach, and is ideally suited for stability computations of systems involving a large number of degrees of freedom.

To alleviate the computational or experimental burden associated with the application of Floquet theory, approximation to the transition matrix can be constructed, based on a small set of excitations, E, and responses (computed or measured), R, of the system; typically these matrices are rectangular because few excitations and measurements are available. Selection of the excitation and measurement variables is critical to the success of this methodology. Excitations and responses are related to the transition matrix, $R = \Phi(t, T)\ E$. However, this relationship does not allow the computation of the transition matrix because E is, in general, not invertible. Various strategies can be used to extract an approximation to the transition matrix based on least square techniques or the singular value decomposition [15,16,17]. Such an approach is applicable to both numerical and experimental studies.

The goal of this paper is to develop a robust methodology for the stability analysis of large dynamical systems modeled with finite element based multibody formulations. The only approach that gives information about *nonlinear stability* is the Lyapunov function method. Clearly, this method cannot be applied to large dimensional numerical models. Hence, the problem of linearized stability is addressed in this paper, *i.e* the stability of small perturbations about a nonlinear equilibrium configuration that could be periodic. For large multibody models, a formal linearization is difficult and costly to obtain for constant in time systems, and virtually impossible in the case of periodic systems. Hence, the only option is to study the response of the system to small perturbations about an equilibrium configuration using a fully nonlinear, multibody formulation. This means, in effect, that the complex dynamic model is used as a virtual prototype of the actual dynamical system, and the analyst is running a set of "experiments" to determine the stability characteristics of the system. Consequently, it is instructive to investigate the performance of the methods

that have traditionally been used for experimental problem and assess their applicability to numerical models of complex systems.

In this framework, the actual sensors that experimentally measure the response of a physical system are replaced by "sensors" that extract from the numerical model the predicted response of the system. In an experimental setting, stability analysis methods must be robust enough to deal with experimental noise. Numerical implementation also involves noise associated with the time discretization and inaccuracies of the solution. Another source of noise is the fact that the computed response is not that of a linear system, but rather that of a nonlinear system acted upon by small perturbations. In practice, this is a major hurdle: if the perturbation is too large, the nonlinearity in the response is pronounced and linearized stability tools give erroneous stability characteristics; on the other hand, if the perturbation is too small, the response has a small amplitude that becomes indistinguishable from the numerical noise, leading once again to erroneous predictions. This discussion clearly indicates that noise is as much a problem for numerical methods as it is for experimental methods. In the following paragraphs, methods used for stability analysis in experimental settings are reviewed.

The Ibrahim time domain method [18,19] was introduced as a means of extracting damping rates and stability information from experimental measurements. In this approach, the system is excited and responses are measured so that a large number of measurements in time are available. Then, the responses of the system $\underline{X}((k-1)\ T)$ and $\underline{X}(kT)$ serve as k^{th} excitation and measurement, respectively, in the framework of Partial Floquet theory. Hence, The Ibrahim time-domain method is a special case of the partial Floquet approach.

The complex exponential method [19], also known as Prony's method, is generally viewed as a curve fitting procedure. The measured response of a linear periodic system is fitted to the form predicted by Floquet theory, eq. (1). This approach will be further developed in this paper, and the close relationship of Prony's method to Floquet and partial Floquet theories will be proved.

The moving block method [20,21] is another curve-fitting technique that is widely used for experimental data reduction. This method appears to be a pure curve fit method and does not seem to be related to the other approaches described earlier. Although it can yield useful stability information, the results are quite sensitive to many of the parameters of the methods and details of its implementation.

In view of the above discussion, it seems desirable to study the applicability of experimental methods to numerical problems. The most powerful methods for experimental stability analysis of periodic systems appear to be the partial Floquet and Prony's methods. The Ibrahim time domain method is a special case of the partial Floquet method, and hence, will not be considered here. The moving block does not seem to be as robust as the other two, specially in the presence of nonlinearities and closely spaced frequencies. The first contribution of this paper is to show that the partial Floquet and Prony's methods are, in fact, nearly identical. Consequently, Prony's method is not a curve fitting process, but rather a method based on a rigorous procedure for stability analysis, Floquet theory. Second, this observation

allows the development of a robust procedure that is equally applicable to experimental and numerical problems.

3 The Sampled Data

Since the methods developed in this work are inherited from experimental techniques, they are based on "sampled data" obtained from experimental measurements or numerical simulations of the system. Consider a linear system featuring coefficients that are periodic in time with a period T. According to Floquet theory [4], the response of a degree of freedom of the system can be written as

$$h(t) = \sum_{i=0}^{N-1} A_i(t)\ e^{\lambda_i t}, \tag{2}$$

where N is the order of the system, λ_i its characteristic exponents, and $A_i(t) = A_i(t+T)$ are periodic functions. Eq. (2) assumes that the characteristic exponents of the system are all distinct. In the presence of multiple exponents, the response of the system can still be written in closed form, see ref. [4], but the present developments assume that the system features distinct exponents.

The response of the system is sampled at a constant rate Δt, such that $T = p\ \Delta t$, where $p > 1$ is an integer. The following notation is used to identify the sampled data points

$$h_{k,\ell} = h(t = k\Delta t + \ell T), \tag{3}$$

and this convention is illustrated in fig. 1. In the following developments, it will be necessary to work with sequences of m consecutive data points starting at time $t = kT$, that will be stored in the following array

$$\underline{h}_\ell^T = \lfloor h_{0,\ell}, h_{1,\ell}, h_{1,\ell}, \ldots, h_{m-1,\ell} \rfloor. \tag{4}$$

Let μ be an integer such that $0 < \mu < p$ and ν an integer such that $\nu > 1$. Array $\underline{h}_\ell$ lists a sequence of data points spanning less than one period of the system if $m = p - \mu$, spanning exactly one period if $m = p$, spanning more than one period if $m = p + \mu$, or even several periods if $m = \nu p + \mu$. Two matrices will play an important role in subsequent developments

$$H_0 = [\underline{h}_0, \underline{h}_1, \underline{h}_2, \ldots, \underline{h}_{N-1}], \tag{5}$$

and

$$H_1 = [\underline{h}_1, \underline{h}_2, \underline{h}_3, \ldots, \underline{h}_N]. \tag{6}$$

Each column of these matrices stores an array $\underline{h}_\ell$, as defined by eq. (4), *i.e.* a sequence of m consecutive data points.

If the sampled data is the response of a linear periodic system, it must be in the form of eq. (2), implying that

$$h_{k,\ell} = \sum_{i=0}^{N-1} A_i(k\Delta t + \ell T)\ e^{\lambda_i(k\Delta t + \ell T)}. \tag{7}$$

With the help of the following notation, $q_i = e^{\lambda_i \Delta t}$ and

$$Q_i = e^{\lambda_i T} = q_i^p, \tag{8}$$

this expression becomes

$$h_{k,\ell} = \sum_{i=0}^{N-1} q_i^k Q_i^\ell A_i(k\Delta t), \tag{9}$$

where the periodicity of the function $A_i(t)$ implies that $A_i(k\Delta t + \ell T) = A_i(k\Delta t)$.

One approach to stability analysis is to determine the characteristic exponents, λ_i, of the system from the knowledge of sampled data point, $h_{k,\ell}$. If a sufficient number of data points are available, eq. (9) could be used to compute those characteristic exponents. This task is, however, difficult because the equations are nonlinear, and because of the noise that will be undoubtable present in the sampled data.

4 Prony's Method

Prony's method [19] is a procedure that determines the characteristic exponents, λ_i, of a periodic system, based on the knowledge of a set of data points, see eq. (3), sampled from the system output. To that effect, a linear combination of the data points is formed

$$\begin{aligned}\sum_{\ell=0}^{N-1} \beta_\ell h_{k,\ell} + h_{k,N} &= \sum_{\ell=0}^{N-1} \beta_\ell \sum_{i=0}^{N-1} q_i^k Q_i^\ell A_i(k\Delta t) + \sum_{i=0}^{N-1} q_i^k Q_i^N A_i(k\Delta t), \\ &= \sum_{i=0}^{N-1} q_i^k A_i(k\Delta t) \left[\sum_{\ell=0}^{N-1} \beta_\ell Q_i^\ell + Q_i^N \right],\end{aligned} \tag{10}$$

where the coefficients β_ℓ are as yet unknown coefficients. The linear combination of the data points defined by eq. (10) can be made to vanish if the bracketed terms in the last expression all vanish, *i.e.* if

$$\beta_0 + \beta_1 Q_i + \beta_2 Q_i^2 + \ldots + \beta_{N-1} Q_i^{N-1} + Q_i^N = 0, \quad i = 0, 1, 2, \ldots, N-1. \tag{11}$$

These conditions are satisfied if and only if the Q_i are the N roots of the N^{th} order polynomial defined by the coefficient β_i,

$$\beta_0 + \beta_1 Q + \beta_2 Q^2 + \ldots + \beta_{N-1} Q^{N-1} + Q^N = 0. \tag{12}$$

With this choice of the Q_i, the linear combination defined in eq. (10) then reduces to $\sum_{\ell=0}^{N-1} h_{k,\ell}\beta_\ell + h_{k,N} = 0$. The same reasoning can be made for any value of index $k = 0, 1, 2, \ldots, m-1$. Collecting all results then yields

$$\sum_{\ell=0}^{N-1} h_{k,\ell}\beta_\ell = -h_{k,N}, \quad k = 0, 1, 2, \ldots, m-1. \tag{13}$$

These equations form a *set of linear equations* for the unknown coefficients β_i. With the help of the following notation

$$\underline{\beta}^T = \lfloor \beta_0, \beta_1, \beta_2, \ldots, \beta_{N-1} \rfloor \tag{14}$$

the system of linear equations, eq. (13), can be recast as

$$H_0 \, \underline{\beta} = -\underline{h}_N, \tag{15}$$

where matrix H_0 was defined in eq. (5). In general $m > N$, and this system is an over determined set of linear equations that could be solved using the least square method [22], for instance.

Prony's method can be summarized as a three step process. First, using the sampled data, form the array $\underline{h}_N$ and matrix H_0 defined by eqs. (4) and (5), respectively. Next, solve the linear system defined by eq. (15) to find the N coefficients β_i. If necessary, *i.e.* if $m > N$, use an appropriate method to determine an approximate solution of the over determined linear system. Finally, determine the N roots, Q_i, of the polynomial defined by eq. (12). The characteristic exponents of the system are then obtained from the definition of Q_i, see eq. (8).

The second step of the procedure can present difficulties: as the order of the system increases, so does the order of the polynomial defined by eq. (12) and the extraction of its root becomes an increasingly arduous task. One of the most reliable manners of computing the roots of a polynomial [23,24] is to recast the problem as an eigenvalue problem. To that effect, the following matrix relationship is constructed

$$\lfloor 1, Q, Q^2, \ldots, Q^{N-1} \rfloor \begin{bmatrix} 0 & 0 & \ldots & 0 & -\beta_0 \\ 1 & 0 & \ldots & 0 & -\beta_1 \\ 0 & 1 & \ldots & 0 & -\beta_2 \\ 0 & 0 & \ddots & \vdots & \vdots \\ 0 & 0 & \ldots & 0 & -\beta_{N-2} \\ 0 & 0 & \ldots & 1 & -\beta_{N-1} \end{bmatrix} = Q \lfloor 1, Q, Q^2, \ldots, Q^{N-1} \rfloor, \tag{16}$$

where the first $N-1$ equations are identities, whereas the last equation is identical to the

polynomial equation defined by eq. (12). The following notation is introduced

$$B = \begin{bmatrix} 0 & 0 & \dots & 0 & -\beta_0 \\ 1 & 0 & \dots & 0 & -\beta_1 \\ 0 & 1 & \dots & 0 & -\beta_2 \\ 0 & 0 & \ddots & \vdots & \vdots \\ 0 & 0 & \dots & 0 & -\beta_{N-2} \\ 0 & 0 & \dots & 1 & -\beta_{N-1} \end{bmatrix}; \quad \underline{\mathcal{Q}} = \begin{bmatrix} 1 \\ Q \\ Q^2 \\ \vdots \\ Q^{N-1} \end{bmatrix}, \tag{17}$$

where matrix B is an upper Hessenberg matrix known as the *companion matrix to a polynomial*. Eq. (16) now simply writes

$$B^T \underline{\mathcal{Q}} = Q \underline{\mathcal{Q}}. \tag{18}$$

This is clearly a standard eigenvalue problem; the eigenvalues, Q, of matrix B are also the roots of the polynomial defined by eq. (12). The eigenvalues of B are, in general, complex conjugate numbers, since all β_i are real numbers. It will be convenient to write

$$Q_i = r_i e^{\pm j\phi_i}, \tag{19}$$

where $j = \sqrt{-1}$.

The last step of Prony's method involves the determination of the characteristic exponents of the system from the eigenvalues, Q_i, of matrix B. The characteristic exponents will be written in the following form

$$\lambda_i = \omega_i \left[\zeta_i \pm j\sqrt{1-\zeta_i^2} \right], \tag{20}$$

where the ω_i and ζ_i are the frequency and damping, respectively, associated with this characteristic exponent. In view of eq. (8), it then follows that

$$\zeta_i = \sqrt{\frac{c_i^2}{1+c_i^2}}; \quad \omega_i = \frac{c_i \phi_i}{\zeta_i T}, \quad i = 0, 1, 2, \dots, N-1, \tag{21}$$

where $c_i = (\ln r_i)/\phi_i$.

4.1 Relationship to Floquet Theory

The linear system defined by eq. (15) can be expanded to form the following matrix relationship

$$[\underline{h}_0, \underline{h}_1, \underline{h}_2, \ldots, \underline{h}_{N-1}] \begin{bmatrix} 0 & 0 & \ldots & 0 & -\beta_0 \\ 1 & 0 & \ldots & 0 & -\beta_1 \\ 0 & 1 & \ldots & 0 & -\beta_2 \\ 0 & 0 & \ddots & \vdots & \vdots \\ 0 & 0 & \ldots & 0 & -\beta_{N-2} \\ 0 & 0 & \ldots & 1 & -\beta_{N-1} \end{bmatrix} = [\underline{h}_1, \underline{h}_2, \underline{h}_3, \ldots, \underline{h}_N] \,. \tag{22}$$

Note that the first $N-1$ equations implied by this relationship are identities, $\underline{h}_1 = \underline{h}_1$, $\underline{h}_2 = \underline{h}_2$, etc., whereas the last equation is identical to the linear system of eq. (15). Using the notation defined in eqs. (5), (17) and (6), this matrix equation simply writes $H_0 B = H_1$. Transposing this relationship yields

$$H_1^T = B^T H_0^T. \tag{23}$$

The columns of matrix H_0^T store excitations of the system and the columns of H_1^T the corresponding responses one period later. This implies that matrix B^T is the *Floquet transition matrix of the system*, that could be computed from the sampled data as $B^T = H_1^T H_0^{-T}$. In fact, if N linearly independent excitations are available, H_0 is an invertible matrix and this relationship would yield the exact Floquet transition matrix of the system. A fundamental result of Floquet theory [4,5] is that the eigenvalues of this transition matrix are the Q_i defined by eq. (8). This result is identical to that obtained in the derivation of Prony's method: the Q_i are the eigenvalues of the companion matrix B. This proves that Prony's method is not simply a curve fitting methods; rather, it is closely related to Floquet theory, a rigorous tool for the stability analysis of linear periodic systems.

Since Prony's and partial Floquet methods are equivalent, it is not unexpected that both methods require the inverse of the same matrix H_0, as implied by eqs.(15) and (23), respectively. Since H_0 is not necessarily a square matrix, and not necessarily of full rank, its inverse does, in general, not exist, a problem that is closely related to the noise and redundancy in the sampled data. Although Prony's and partial Floquet methods are equivalent, practical implementations of Prony's method are computationally more elegant and efficient because it requires the identification of array $\underline{\beta}$ of size N, whereas the partial Floquet method requires the identification of the transition matrix B of size N^2. Hence, the practical implementation of the sole Prony's method will be addressed next.

5 Practical Implementation

To be effective in the stability analysis of large multibody systems, the details of the implementation of the method described in the previous section must be carefully considered. In applications of Prony's method to experimental set-ups, a limited number of signals are available, because each signal requires a physical sensor, adding to the cost and complexity of the experiment. On the other hand, in numerical applications, comprehensive dynamical models typically involve a large number of degrees of freedom and hence, a large number of "sensors" are available at no cost. This fact is a double edged sword; as the number of sensors increases, more robust predictions should be obtained because more data is readily available, but the highly redundant data leads to an increasingly ill conditioned and rank deficient system of equations (15).

If N_s signals are used for stability analysis, the following arrays are constructed

$$\mathbb{H}_0 = \begin{bmatrix} H_0^{(1)} \\ H_0^{(2)} \\ \vdots \\ H_0^{(N_s)} \end{bmatrix}; \quad \underline{\mathcal{H}}_N = \begin{bmatrix} \underline{h}_N^{(1)} \\ \underline{h}_N^{(2)} \\ \vdots \\ \underline{h}_N^{(N_s)} \end{bmatrix} \tag{24}$$

where $H_0^{(k)}$ and $\underline{h}_N^{(k)}$ are the matrix and array constructed with the data of the k^{th} signal, as defined by eqs. (5) and (4), respectively. Prony's method now involves the solution of the following linear system

$$\mathbb{H}_0 \, \underline{\beta} = \underline{\mathcal{H}}_N, \tag{25}$$

where $\mathbb{H}_0$ is a matrix of size $mN_s \times N$ and $\underline{\mathcal{H}}_N$ an array of size mN_s. Of course, each signal should be normalized prior to forming matrix $H_0^{(k)}$ and array $\underline{h}_N^{(k)}$.

The main difficulty of practical implementations of Prony's method is the determination of the order, N, of the system. From a theoretical standpoint, the order of the system equals its number of degrees of freedom, typically a very large number for comprehensive multibody models. However, the available data is unlikely to be sufficient to identify all the characteristic exponents of the system. Indeed, Floquet theory implies that the determination of the N characteristic exponents requires a complete knowledge of the transition matrix, which in turns, requires the evaluation of the system response to N linearly independent initial conditions. If such data were to available, Prony's and Floquet methods would become identical, and would both yield all the characteristic exponents of the system. In practical situations, it is reasonable to ask the following question: given the sampled data available for the analysis, how many characteristic exponents can be accurately computed?

Let N' denote a preliminary estimate of the observable order of the system that will be evaluated based on two criteria. First, the system of equations (25) should be over determined, *i.e.* $mN_s = \alpha N'$, where $\alpha > 1$ is a user defined parameter. Second, it is desirable to use as much of the available data as possible, *i.e.* $pN' + m - 1 = N_d - 1$, where N_d is the total

number of data points in a signal. Solving these two equations yields

$$N' = \frac{N_s N_d}{\alpha + pN_s}, \quad m = \frac{\alpha N_d}{\alpha + pN_s}. \tag{26}$$

With this choice, system (25) represents an over determined system of linear equations that could be solved using the least square method [22], for instance. This approach, however, does not guarantee an accurate solution because $\mathbb{H}_0$ could still be rank deficient due to the redundant nature of the sampled data. Hence, the singular value decomposition technique [22] is used to first determine the rank of $\mathbb{H}_0$. This decomposition implies that $\mathbb{H}_0$ is factorized as $\mathbb{H}_0 = U\text{diag}(\sigma_i)V^T$, where U and V are orthogonal matrices and $\text{diag}(\sigma_i)$ a real diagonal matrix such that $\sigma_1 \geq \sigma_2 \geq \ldots \sigma_N \geq 0$. The rank r of the matrix is then determined by the following condition

$$\frac{\sigma_1}{\sigma_1} \geq \frac{\sigma_2}{\sigma_1} \geq \ldots \frac{\sigma_r}{\sigma_1} \geq \varepsilon_{\text{rank}} \geq \ldots \frac{\sigma_s}{\sigma_1} \geq \varepsilon_{\text{noise}} \geq \ldots \frac{\sigma_N}{\sigma_1} \geq 0, \tag{27}$$

where $\varepsilon_{\text{rank}}$ and $\varepsilon_{\text{noise}}$ are user defined tolerances. This analysis indicates that r characteristic exponents can be reliably extracted from the given data, but that s characteristic exponents are present in the response. The remaining characteristic exponents should be treated as noise.

With this information at hand, linear system (25) is formed with $\mathbb{H}_0$ of size $mN_s \times s$, where $m = N_d - ps$. This yields an array $\underline{\beta}$ of size s, and s characteristic frequencies and damping rates can then be evaluated with the help of eq. (21). Of these s damping rates, r only should be considered to be reliable estimates, typically those with the lowest rates.

6 Numerical Examples

In all numerical examples presented below, the following values of the user defined parameters were used: $\alpha = 2$, $\varepsilon_{\text{rank}} = 10^{-3}$ and $\varepsilon_{\text{noise}} = 10^{-5}$.

6.1 Flutter of a Rectangular Planform Wing

The first example is an aeroelastic problem dealing with the symmetric flutter of a rectangular planform wing clamped at its mid-point [25]. Due to symmetry, a half configuration was modeled and proper symmetry conditions were applied. This problem involves both structural and aerodynamic states. The half wing has a rectangular planform of length $L = 20$ ft and chord length $c = 6$ ft. The flutter speed of the wing was experimentally measured as $U_F = 590$ ft/s.

The structural properties of the cantilevered wing are as follows: bending stiffness, $EI = 2.4\ 10^7$ lbs·ft^2, torsional stiffness, $GJ = 2.4\ 10^6$ lbs·ft^2, mass per unit span, $m = 0.75$ slugs/ft,

polar moment of inertia, $I = 1.95$ slugs·ft. The airfoil quarter-chord and center of mass are located 0.5 and 0.6 ft aft the elastic axis of the wing, respectively. The wing semi-span is modeled with four cubic beam elements.

The aerodynamic model combines thin airfoil theory with a three dimensional dynamic inflow model. The airfoil has a constant slope of the lift curve $a_0 = 6.28$, and the moment coefficients about the quarter-chord are zero. The inflow velocities at each span-wise location are computed using the finite state induced flow model developed by Peters *et al.* [26,27]. The number of inflow harmonics was selected as $m = 9$, corresponding to 55 aerodynamic inflow states for this symmetric problem. Airloads were computed at 9 stations along the wing span, located at the positions corresponding to Gaussian quadrature. Selecting a larger number of aerodynamic states or airloads computation points did not significantly affect the results.

The simulation was run for a total period of 1 s, using a constant time step $\Delta t = 10^{-3}$ s. Two cases will be contrasted in this example. The first case, denoted *case 1*, uses two signals: the three-quarter span transverse displacement and twist of the wing; the second case, denoted *case 2*, uses four signals: the three-quarter span transverse displacement and twist of the wing, and its root bending moment and torque. Fig. 2 shows the frequency and damping of the two modes with the lowest frequencies versus far field flow velocity. This figure is similar to that obtained from the classical, two degree of freedom analysis of a wing section [28]. The lowest bending and torsional modes nearly coalesce at flutter. Note that the higher bending and torsional modes do not appear on the figure, although they are included in the model. This is due to the fact that these modes are heavily damped by the aerodynamic forces, and hence are identified as "noise" by Prony's method. To illustrate this point, fig. 3 shows the normalized singular values of matrix $\mathbb{H}_0$ for *cases 1* and *2*. When two sensors only are used, six singular values only are larger than $\varepsilon_{\text{rank}}$ whereas when four sensors are used, the additional data enables the accurate estimate of twelve singular values. This means that in *cases 1* and *2*, a system of order six and twelve, respectively, will be identified.

From fig. 2, the flutter speed is found to be $U_F = 585$ ft/s, for *cases 1* and *2*; this compares favorably with the experimentally measured flutter speed of 590 ft/s. For *case 2*, the additional two sensors allow a more accurate determination of the frequency and damping rates, as demonstrated by the smoother curves shown in fig. 2. It should be noted, however, that both cases predict the same flutter speed. The predictions becomes less accurate in the unstable regime, due to the nonlinear behavior associated with large deflections of the wing. Furthermore, it becomes increasingly difficult to trace the second mode because it is heavily damped.

6.2 The wind turbine problem

The second example deals the modeling of the three-bladed wind turbine depicted in fig. 4. The physical properties of the system are tabulated in ref. [29] and will not be repeated here. In the multibody dynamics model [8], the cantilevered tower is connected to a flexible

bed plate, modeled with two and one cubic beam elements, respectively. The shaft, modeled as a single cubic beam element, is connected to the bed plate by means of a revolute joint. In turns, the tip of the shaft is attached to the hub, modeled as a rigid body. Finally, the three flexible blades, each modeled by two cubic beam elements, are attached to the hub by revolute joints, called "lag hinges," that allow relative rotation of the blade with respect to the hub in the plane of rotation of the rotor and flexible root retention beams, each modeled as a single cubic beam element, connect the assemblies back to the hub.

As the angular speed of the rotor increases, an instability of a purely mechanical origin is encountered in this periodic system. It is associated with a coupling between the motions of the blades in the plane of rotation of the rotor and lateral vibrations of the tower. If the blades are considered to be rigid bodies and the tower replaced by an equivalent spring-mass system, it is possible to find an analytical solution of the problem: the governing equations with periodic coefficients are transformed to a set of equations with constant coefficients using a Fourier transformation, and classical methods are then used to predict linearized stability. On the other hand, the multibody model was used to predict the dynamic response of the system for various rotor speeds. A small perturbation, in the form of a triangular impulsive moment (total duration: 0.05 s; maximum amplitude 10^4 N·m) acting at the lag hinge of the first blade, was used to excite the system. Its stability was then assessed using Prony's method with a total of seven sensors: the two tip transverse deflections of the tower, the two root bending moments of the tower, and the three relative rotations at the lag hinges of blades. The predicted damping in the system is shown in fig. 5: the unstable region extends from about 9.4 to 11.3 rad/s rotor speed. For reference, the analytical solution obtained from the approximate, rigid body model is also shown in the figure; although the damping rates predicted by the two models are slightly different, as expected, the predicted instability boundaries are in close agreement. Two other simulations were performed by removing one and two of the lag hinge dampers, respectively; the results are also shown in fig. 5. It is interesting to note that the loss of one or two dampers does not significantly alter the stability characteristics of the system. It should also be noted that when the damping of the system nearly vanishes, *i.e.* near the stability boundaries, the following user defined parameters has to be modified as: $\varepsilon_{\text{rank}} = 10^{-5}$ and $\varepsilon_{\text{noise}} = 10^{-7}$. Indeed, it is inherently more difficult to measure very small amounts of damping because they generate small amplitude differences from cycle to cycle that are obscured by experimental noise.

6.3 Stability Analysis of a soft in-plane tilt rotor system

The last example deals with a detailed analysis of a soft in-plane tilt rotor system [30] using a finite element based multibody dynamics code [8]. This multibody representation includes the rotor blades, pitch link, pitch horns, swash plate (rotating and non-rotating components), and hydraulic control actuators, see fig. 6, which are attached to an elastic wing through the pylon, see fig. 7. The rotor blades are modeled as elastic beams undergoing coupled flap, lag and torsion deformations.

Figure 6 illustrates the key elements of the multibody model of the tilt rotor. The wing, rotor mast, and four blades are modeled as elastic beam elements featuring four parabolic, five cubic and one cubic element, respectively. The aerodynamic forces on rotor and wing are modeled using lifting line theory; rotor inflow is calculated with a three-dimensional nonlinear dynamic inflow model [27]. Aerodynamic interactions between the rotor and wing are ignored. The rotor hub, pitch links/horns, swash plates, and pylon are modeled as rigid bodies. The blade flap and lag hinges and torsion bearings are modeled as revolute joints; the stiffness and damping of the blade lag damper are included in the lag revolute joint element. The pylon conversion actuators are modeled as flexible joints, *i.e.* a set of concentrated springs and dampers. Two configurations of the tilt rotor in airplane mode were tested in the wind tunnel: the off-downstop configuration, which simulate the pylon conversion actuator stiffness and damping in conversion state, and the on-downstop configuration, which has higher actuator stiffnesses to simulate the "locked" state after conversion to airplane mode. It is important to model these two pylon conversion actuators accurately because they determine the wing chordwise/torsional mode frequency, and this mode is critical in tilt rotor aeroelastic stability.

The very complex system described above will be used to illustrate the proposed stability analysis tool in two manners. First, the *experimental measurements* will be processed to extract frequencies and damping rates using three different approaches. Second, the dynamic response of the system will be predicted based on the multibody model described above. Prony's method will then be used to extract the frequencies and damping rates of the system from its *predicted response*; these predictions will then be compared with the experimental measurements.

For nominal parameter values of 550 rpm rotor speed and 25 knot airspeed, four experiments, labelled #4190 to #4193, were run in the off-downstop configuration. The system was excited during a short time with a shaker, and strain gauges were used to measure wing root bending moments upon completion of the excitation. This experimental signal will be used to extract frequencies and damping rates of the system using three approaches: the moving block, Prony's and partial Floquet methods. In each case, four window sizes were used to analyze the signal corresponding to 3/4, 4/5, 5/6 and 7/8 of the total experimental record. Table 1 lists the average frequencies and corresponding coefficients of variation extracted from this data using the three methods; system damping rates are listed in table 2. Note that smaller coefficients of variation were obtained when extracting frequencies with Prony's and partial Floquet methods than with the moving block approach. On the other hand, all three methods exhibit larger coefficients of variation when it comes to damping rates. This is due to the small amount of damping present in the system, of the order of 3%: a small amount of damping is inherently difficult to measure because it generates small amplitude differences from cycle to cycle that are obscured by experimental noise. For damping rates, the coefficient of variations computed based on the four nominally identical experiments are larger than those obtained for four windows of the same signal; this indicates that the experimental error is mainly due to the experimental set-up, rather than to the damping identification procedure. System characteristics identified by the three methods are in good agreement with each other. This should be expected from Prony's and partial Floquet methods, since they are closely related to each other, as explained above. The moving block also performed satisfactorily because

its main shortcomings [20,21] did not affect its prediction for this particular experiment.

During wind tunnel testing, the variation of wing beamwise damping in airplane-mode was investigated as a function of rotor torque, *i.e.* as a function of rotor collective angle. As shown in fig. 8, the test data exhibits dramatic nonlinear damping variations for rotor collective angles over the range of 10 to 15 degrees. For larger rotor collective angles, wing beamwise damping shows an expected, nearly linear increase with collective angle. In the same range of collective angles, rotor torque is known to be small, with a zero torque crossing, the so called "wind milling" case, at about 14 degrees. When rotor torque is slightly shifted from zero, in the positive or negative directions, wing beamwise damping exhibits a sharp increase, or shoulder, well above the damping measured for larger rotor mast torque values. This nonlinear variation in wing beamwise damping for small rotor torque values may be attributed to the coupling of rotor, wing and drive train dynamics. Drive train free-play increases this coupling and renders it highly nonlinear. To prove this point, three models with different levels of fidelity were exercised, labelled *case 1* to *3*. *Case 1* ignored drive train dynamics, *i.e.* the rotor mast was modeled as a rigid body; *case 2* included an elastic rotor mast, modeled as a beam with a torsional stiffness that matches that of the drive train system; finally, in *case 3*, the rotor mast is connected to the hub by means of a revolute joint with backlash [31] featuring a ± 1 degree free-play angle.

Figure 8 shows the predictions of the analysis for the three different models; in all cases, damping rates were extracted from the numerical predictions using Prony's method. The two models that ignore free-play do not capture the nonlinear relationship between collective angle and beamwise wing damping. On the other hand, with the inclusion of free-play, both lowest damping point (wind milling case) and the sharp increase in damping near the zero torque point are well captured by the model. It is interesting to note that the phenomenon under scrutiny in this example, intermittent contact due to free-play, is inherently nonlinear. On the other hand, all the methods for stability assessment presented in this work are derived based on the assumption of linearity of the system governing equations. Yet, the proposed methods performed well on both experimental and numerical signals. This is probably due to the ability of the proposed method to deal with signal noise: the nonlinear behavior is "filtered out" as if it were noise. This does not imply that Prony's method will always adequately perform in the presence of nonlinearities, but rather that is can, in some cases, give good results.

7 Conclusions

The linearized stability analysis of dynamical systems modeled using finite element based multibody formulations was addressed in this paper. The use of classical methods for stability analysis of these system, such as the characteristic exponent method or Floquet theory, results in computationally prohibitive costs. Hence, a different approach was taken: the applicability to numerical models of the stability analysis tools that are used in experimental settings was investigated. This is a logical implication of the fact that comprehensive multi-

body models are "virtual prototypes" of actual systems. The first contribution of this work is a formal proof that Prony's method, generally regarded as a curve fitting method, is equivalent, and sometimes identical, to Floquet theory and to the partial Floquet method. This observation gives Prony's method a sound theoretical footing. The second contribution of this paper is an improved solution procedure for Prony's method that considerably improves the robustness of its predictions when applied to comprehensive models of complex multibody system. In particular, the singular value decomposition technique allows the identification of the order of the system as well as the characteristic exponents, given the available data. Because it is a purely post-processing, *i.e.* signal processing, approach to stability analysis, the proposed approach is equally applicable to experimental and numerical applications. It is computationally inexpensive and can be readily implemented in conjunction with any existing multibody software. Finally, applications of the proposed procedure have been presented that demonstrate its efficiency and limitations for both numerical and experimental applications.

References

[1] V.V. Bolotin. *Nonconservative Problems of the Theory of Elastic Stability.* Pergamon Press Limited, Oxford, England, 1963.

[2] M.J. Goodwin. *Dynamics of Rotor-Bearing Systems.* Unwinm Hyman, London, 1989.

[3] M. Lalane and G. Ferraris. *Rotordynamics Prediction in Engineering.* John Wiley & Sons, New York, 1990.

[4] H. Hochstadt. *Differential Equations.* Dover Publications, Inc., New York, 1964.

[5] A.H. Nayfeh and D.T. Mook. *Nonlinear Oscillations.* John Wiley & Sons, New York, 1979.

[6] A. Cardona. *An Integrated Approach to Mechanism Analysis.* PhD thesis, Université de Liège, 1989.

[7] A. Cardona and M. Géradin. Time integration of the equations of motion in mechanism analysis. *Computers and Structures*, 33(3):801–820, 1989.

[8] O.A. Bauchau, C.L. Bottasso, and Y.G. Nikishkov. Modeling rotorcraft dynamics with finite element multibody procedures. *Mathematical and Computer Modeling*, 33:1113–1137, 2001.

[9] C.S. Hsu. Impulsive parametric excitation: Theory. *Journal of Applied Mechanics*, 39:551–558, 1972.

[10] C.S. Hsu. On approximating a general linear periodic system. *Journal of Mathematical Analysis and Applications*, 45:234–251, 1974.

[11] D.A. Peters and K.H. Hohenemser. Application of the Floquet transition matrix to problems of lifting rotor stability. *Journal of the American Helicopter Society*, 16:25–33, 1971.

[12] P.P. Friedmann, C.E. Hammond, and T.H. Woo. Efficient numerical treatment of periodic systems with application to stability problems. *International Journal for Numerical Methods in Engineering*, 11:1171–1136, 1977.

[13] O.A. Bauchau and Y.G. Nikishkov. An implicit Floquet analysis for rotorcraft stability evaluation. *Journal of the American Helicopter Society*, 46:200–209, 2001.

[14] O.A. Bauchau and Y.G. Nikishkov. An implicit transition matrix approach to stability analysis of flexible multibody systems. *Multibody System Dynamics*, 5:279–301, 2001.

[15] Xin Wang and D.A. Peters. Floquet analysis in the absence of complete information on states and perturbations. In *Proceedings of the Seventh International Workshop on Dynamics and Aeroelasticity Stability Modeling, St. Louis, October 14-16*, 1997.

[16] D.A. Peters and Xin Wang. Generalized floquet theory for analysis of numerical or experimental rotor response data. In *Proceedings of the 24th European Rotorcraft Forum, Marseilles, France, September 15-17*, 1998.

[17] G. Quaranta, P. Mantegazza, and P. Masarati. Assessing the local stability of periodic motions for large multibody non-linear systems using proper orthogonal decomposition. *Journal of Sound and Vibration*, 271:1015–1038, 2004.

[18] S.R. Ibrahim and E.C. Mikulcik. A method for the direct identification of vibration parameters from the free response. *Shock Vibration Bulletin*, 47:183–198, 1977.

[19] D.J. Ewins. *Modal testing: theory and practice*. Wiley, New York, 1984.

[20] C.E. Hammond and Jr. Doggett, R.V. Determination of subcritical damping by moving-block/randomdec applications. In *NASA Symposium on Flutter Testing Techniques, NASA SP-415*, pages 59–76, 1975.

[21] W.G. Bousman and D.J. Winkler. Application of the moving-block analysis. In *Proceedings of the 22th Structures, Structural Dynamics, and Materials Conference, Dallas, TX, April 17-20*, 1981.

[22] G.H. Golub and C.F. Van Loan. *Matrix Computations*. The Johns Hopkins University Press, Baltimore, second edition, 1989.

[23] G. Dahlquist and Å. Björck. *Numerical Methods*. Prentice Hall, Inc., Englewood Cliffs, New Jersey, 1974.

[24] W.H. Press, B.P. Flannery, S.A. Teutolsky, and W.T. Vetterling. *Numerical Recipes. The Art of Scientific Computing*. Cambridge University Press, Cambridge, 1990.

[25] M. Goland. The flutter of a uniform cantilever wing. *Applied Mechanics*, 12(4):A197–A208, 1945.

[26] D.A. Peters, S. Karunamoorthy, and W.M. Cao. Finite state induced flow models. Part I: Two-dimensional thin airfoil. *Journal of Aircraft*, 32:313–322, 1995.

[27] D.A. Peters and C.J. He. Finite state induced flow models. Part II: Three-dimensional rotor disk. *Journal of Aircraft*, 32:323–333, 1995.

[28] R.L. Bisplinghoff, H. Ashley, and R.L. Halfman. *Aeroelasticity*. Addison-Wesley Publishing Company, Reading, Massachusetts, second edition, 1955.

[29] K. Stol, G. Bir, and M. Balas. Linearized dynamics and operating modes of a simple wind turbine model. In *Proceedings of the 37th AIAA Aerospace Sciences Meeting and Exhibit, Jan. 11-14, Reno, Nevada*, pages 135–142, 1999. NICH Report No. 32548.

[30] M.W. Nixon, C.W. Langston, J.D. Singleton, D.J. Piatak, R.G. Kvaternik, L.M. Corso, and R.K. Brown. Aeroelastic stability of a four-bladed semi-articulated soft-inplane tiltrotor model. In *American Helicopter Society 59th Annual Forum Proceedings*, pages 11–25, Phoenix, AZ, May 6-8 2003.

[31] O.A. Bauchau, J. Rodriguez, and C.L. Bottasso. Modeling of unilateral contact conditions with application to aerospace systems involving backlash, freeplay and friction. *Mechanics Research Communications*, 28(5):571–599, 2001.

List of Tables

Experiment ID#	*Moving block*	*Prony*	*Partial Floquet*
#4190	31.979 (0.49%)	32.080 (0.08%)	32.093 (0.10%)
#4191	32.139 (0.37%)	32.193 (0.11%)	32.267 (0.03%)
#4192	32.086 (0.21%)	32.108 (0.06%)	32.142 (0.04%)
#4193	32.014 (0.57%)	32.150 (0.15%)	32.128 (0.09%)
Mean Values	32.055	32.133	32.157
Coefficient of variation	0.22%	0.15%	0.24%

Table 1
Frequencies, in rad/s, (coefficient of variation, in %), extracted from experimental data using the moving block, Prony's, and partial Floquet methods.

Experiment ID#	*Moving block*	*Prony*	*Partial Floquet*
#4190	2.986 (1.65%)	3.070 (0.94%)	3.035 (1.03%)
#4191	3.064 (0.27%)	3.009 (1.88%)	3.006 (0.71%)
#4192	2.797 (1.11%)	2.805 (0.91%)	2.757 (1.88%)
#4193	2.956 (0.31%)	3.044 (1.00%)	3.013 (1.04%)
Mean Values	2.951	2.982	2.953
Coefficient of variation	3.79%	4.05%	4.45%

Table 2
Damping rates, in %, (coefficient of variation, in %), extracted from experimental data using the moving block, Prony's, and partial Floquet methods. Coefficients of variation are indicated in parentheses.

List of Figures

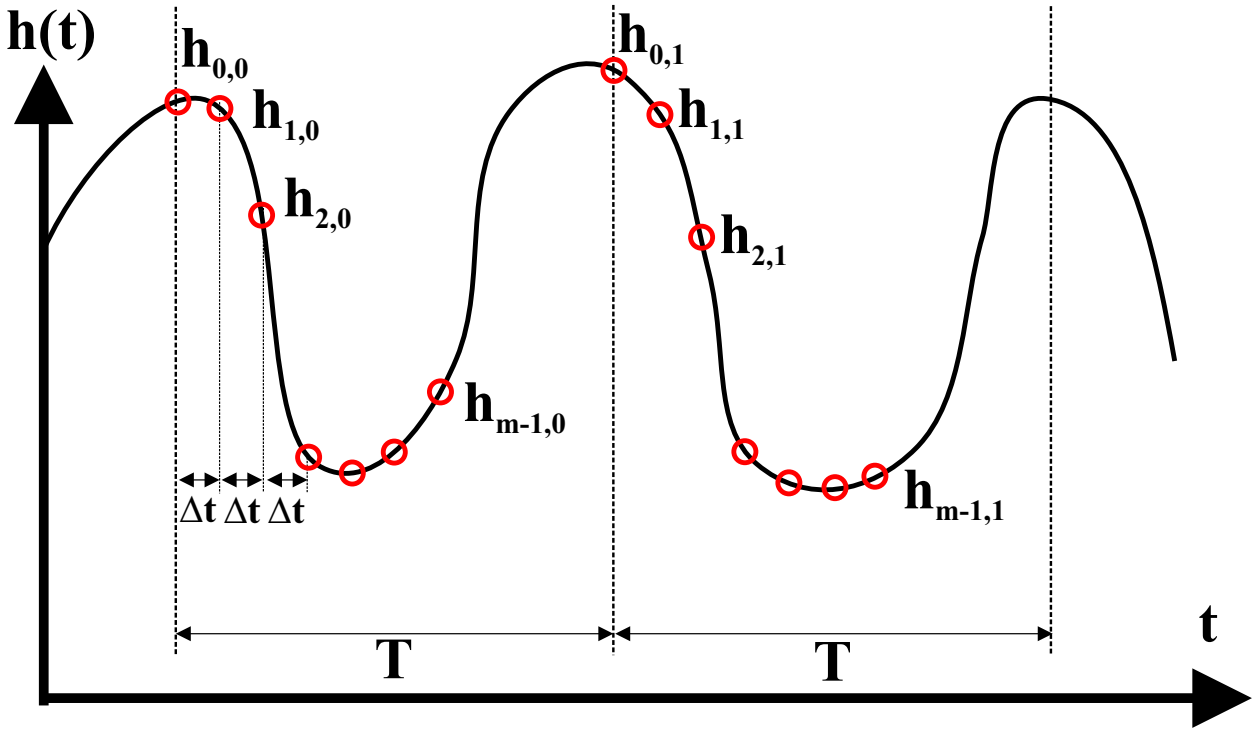

Figure 1. Sampling the output of a periodic system.

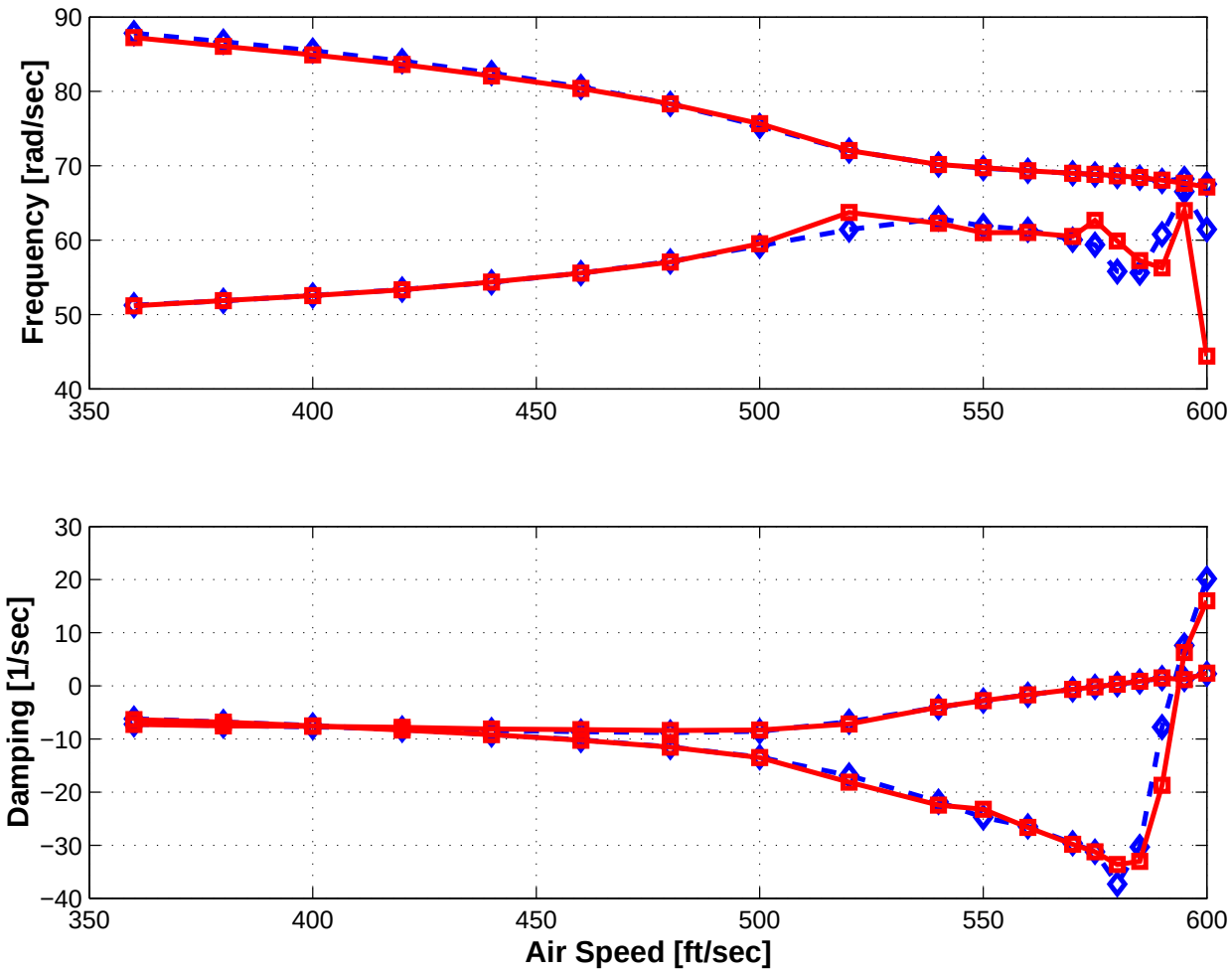

Figure 2. The frequencies and damping of the cantilevered wing. *Case 1*: dashed line (♢); *Case 2*: solid line (□).

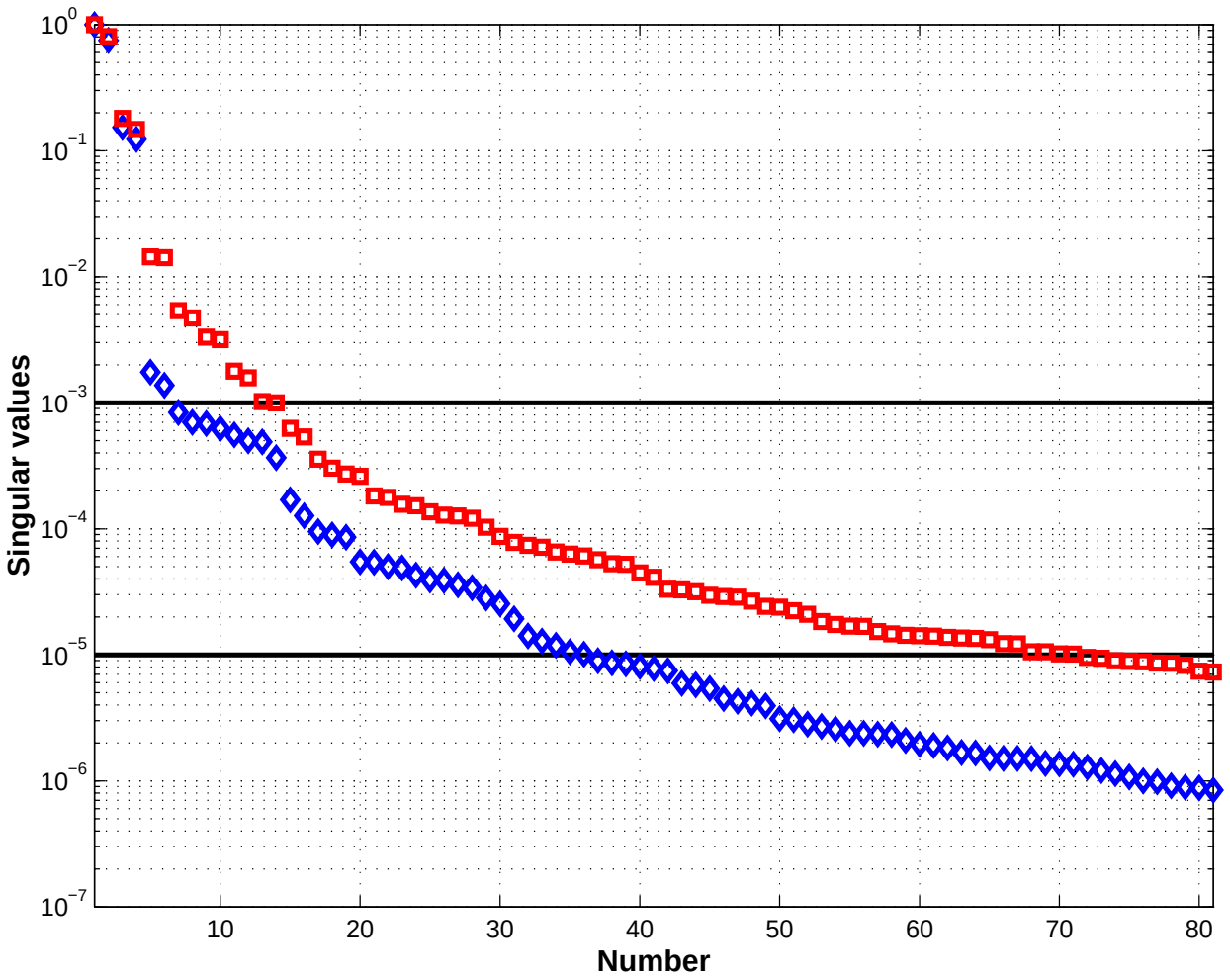

Figure 3. The normalized singular values of matrix $\mathbb{H}_0$ for far field velocity $U = 500$ ft/s. *Case 1*: (♢); *Case 2*: (□). The horizontal lines represent the user defined tolerances: $\varepsilon_{\text{rank}} = 10^{-3}$ and $\varepsilon_{\text{noise}} = 10^{-5}$.

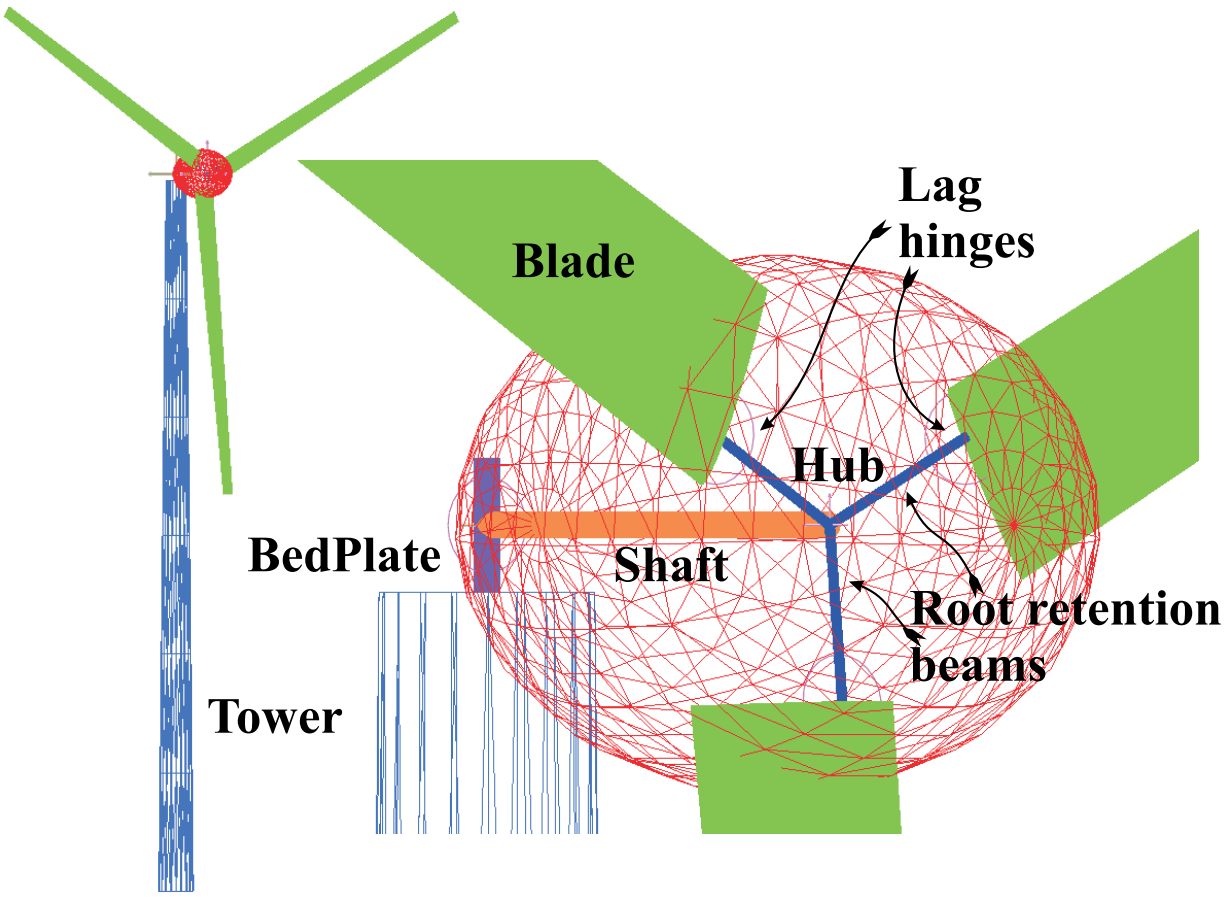

Figure 4. Schematic of the wind turbine problem.

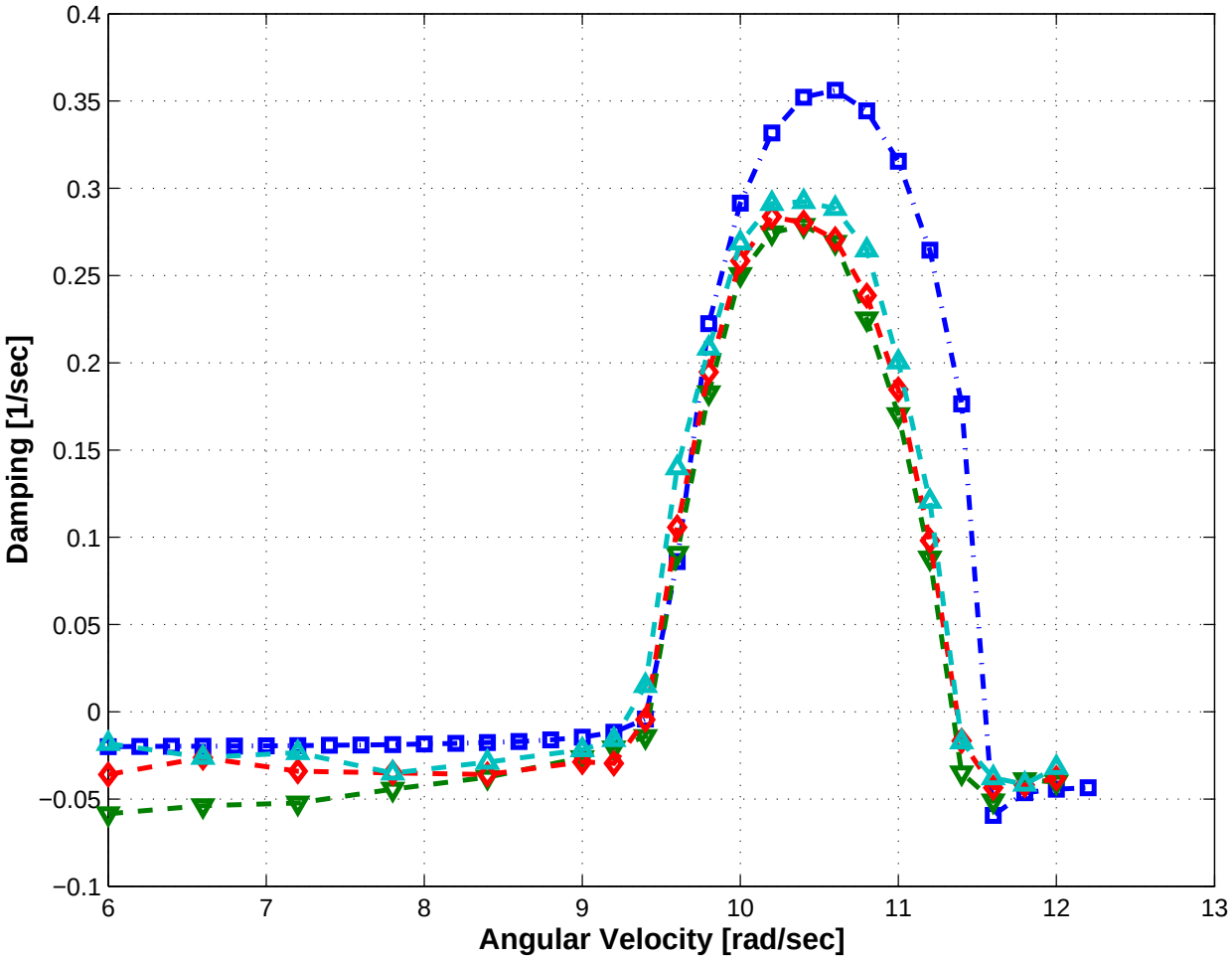

Figure 5. Damping in the wind turbine problem as a function of rotor angular speed. Analytical solution (□); all three dampers active (▽); two dampers active only (◇); single damper active (△).

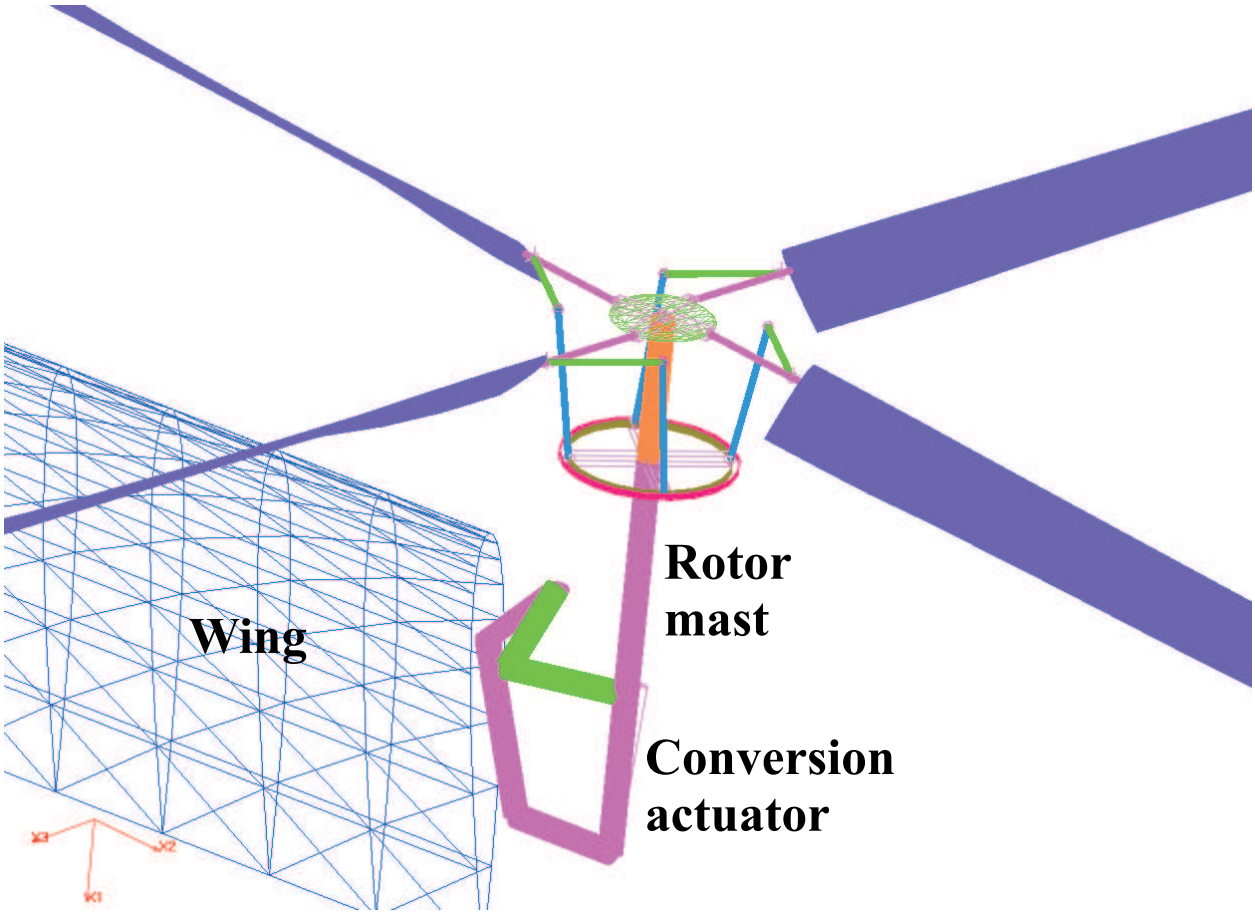

Figure 6. Multibody model of the soft in-plane tilt rotor system.

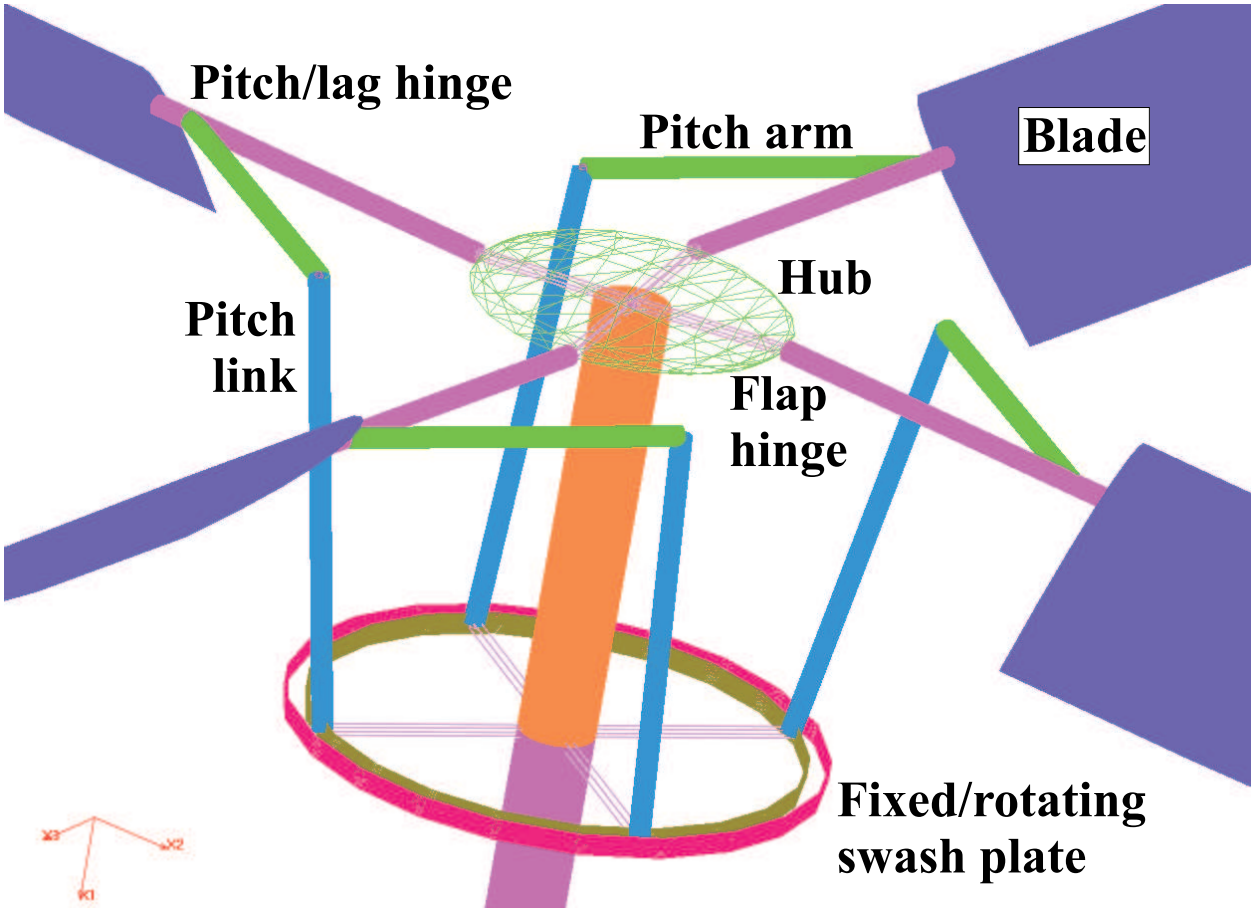

Figure 7. Multibody model of the soft in-plane tilt rotor system: detail of the hub.

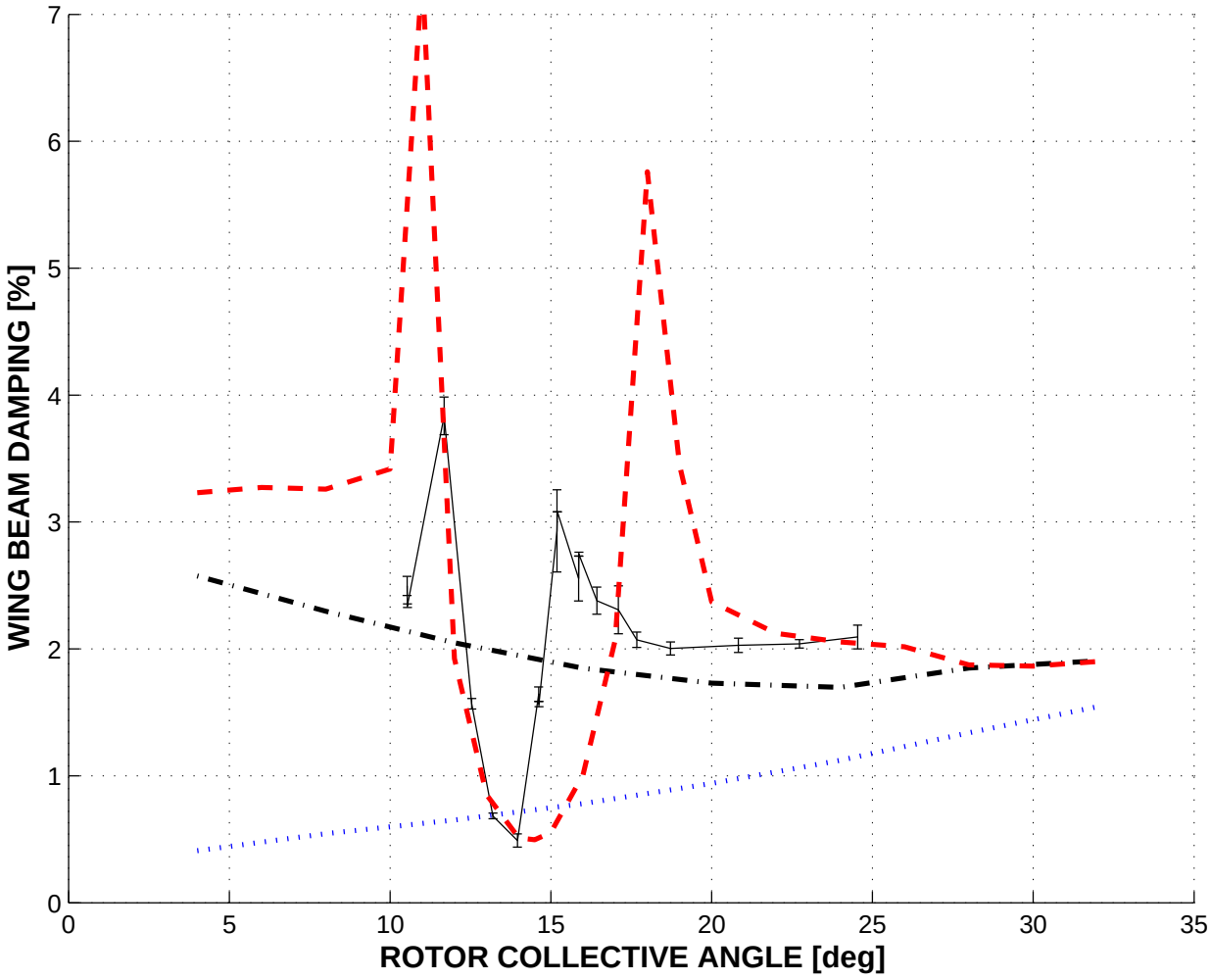

Figure 8. Wing beamwise damping as a function of rotor collective angle; off-downstop configuration, 550 rpm rotor angular speed, 25 knot airspeed. Experimental measurements: solid line; *case 1*: dotted line; *case 2*: dashed-dotted line; *case 3*: dashed line.